Journal of Sound and Vibration (1998) **210**(4), 441–460

VOLUME VELOCITY CONTROL OF SOUND TRANSMISSION THROUGH COMPOSITE PANELS

R. L. St. Pierre, Jr†, G. H. Koopmann and W. Chen

Center for Acoustics and Vibration, *The Pennsylvania State University*, *University Park*, *PA* 16802, *U.S.A.*

(*Received* 4 *March* 1997, *and in final form* 4 *September* 1997)

A design method for minimizing the sound transmitted through an array of panels is presented. This method is based on minimizing the volume velocity of individual segments of the array using integrated control loudspeakers. In this manner, each of the control segments can be treated and controlled separately. The basic acoustic equations governing volume velocity control are presented and it is shown that, at low frequencies, this method achieves global sound power reductions in the far-field. Further analysis shows that this method will achieve significant sound power reductions (10 dB or more) for values of kL of 3·0 or less, where L is the characteristic dimension of each control segment.

Tests conducted in a transmission loss chamber verify the efficacy of volume velocity control using a digital controller. The controller, based on the filtered-X control algorithm, allows for control over a frequency band and results show sound power reductions of 9 dB over a 60 Hz bandwidth. These tests are among the first attempts to use the volume velocity control method over a band of frequencies. The experimental results are complemented by numerical simulations. The results show promise that this methodology is an effective way to control broad band, low-frequency sound transmitted to enclosed spaces, such as airplane or helicopter cabins.

1. INTRODUCTION

Turboprop aircraft have become an important vehicle for short-range travel in the United States, both in the commercial and private sector. These smaller planes are attractive to commercial airline companies because they are less costly and have a lower capacity, making them ideal on less-traveled routes. A common problem in the control of cabin acoustics in this type of airplane is sound transmission at low frequencies, especially the blade passage tones of the propeller. As discussed by Wilby [1] in his excellent overview of research in interior aircraft noise, the blade passing frequency of the propeller and its harmonics are the main contributors of the sound below 400 Hz. Above 400 Hz, boundary layer noise becomes more dominant. Interior sound pressure levels can easily approach 90 dB at low frequencies, where passive sound absorption techniques are, in general, only minimally effective.

Helicopter and rotorcraft cabins are another area where high intensity, low frequency sound is a major problem. In this case the frequencies are generally lower than in turboprop aircraft and the sound levels generally higher. Murray and Wilby [2] show that helicopter noise is significant below 500 Hz where sound pressure levels can exceed 90 dB. Another type of aircraft currently is the tiltrotor which lands and takes off like a helicopter and flies like an airplane, with its propellers perpendicular to the ground. The tiltrotor craft

† Currently at: Cooper Advanced Technologies, Golden, CO 80401, U.S.A.

0022–460X/98/090441 + 20 $25.00/0/sv971306

is being designed for short inter-city transport with the hope that it will take the place of the small commuter turboprop aircraft. However, a major technical challenge in the design of the tiltrotor craft is the high levels of interior noise generated by the propellers at low frequencies.

Because of the high sound levels present at low frequencies in aircraft cabins, active control methods show more promise than attenuating the sound passively. Most of the work described in the open literature uses structural or acoustic actuators to control the sound pressure at designated microphone locations. The strategy presented here attempts to globally reduce sound pressure levels in the interior using only structural sensors on the surface of a vibrating trim panel. In effect, the method controls the acoustic field using only information from the vibrating structure. Therefore, there is no concern about increasing sound pressure levels away from error microphone locations.

The volume velocity control strategy accomplishes this by minimizing the volume velocity of a segment of the vibrating trim panel using an integrated loudspeaker. Accelerometers are used to estimate the volume velocity, which can be thought of as the net displacement of the panel segment. In this way the sound pressure caused by the vibration is ''short circuited'' near the panel's surface without radiating into the interior. Arrays of volume velocity controlled segments can be used to control sound radiated from the parts of the aircraft where the highest vibration levels are seen, typically in the plane of the propellers.

This work is based on converting the vibration of each panel segment into a ''weakly radiating'' mode to reduce the radiated sound, i.e., the volume velocity of a vibration surface is minimized. In this way, the acoustic intensity can be canceled at the surface of the trim panel and global sound reductions in the far-field can be realized. Clark and Fuller [3–5] used a variation of this method using PVDF strips as error sensors and showed that reductions are achieved by shifting the modal energy from the supersonic region in k-space to the subsonic region. This means that much of the acoustic energy remains in the near-field instead of being radiated into the far-field. These papers also explore the optimum locations for sensors and actuators by attempting to focus on modes of vibration that have high radiation efficiencies in the frequency range of interest. Both LQG control and multi-input/multi-output, adaptive, LMS control algorithms are used. Naghshineh and Koopmann [6] developed a numerical algorithm to calculate the control forces necessary to produce this minimum volume velocity condition for a simply supported beam. This method involved directly minimizing the equations for sound power radiated by a baffled beam, determining the necessary control forces. This study also showed that energy is shifted by the optimization to higher wavenumbers and out of the supersonic region in k-space. Johnson and Elliott [7] developed a similar control algorithm for control from a rectangular plate. Their strategy involved reducing the structural velocity into radiation modes instead of vibration modes. These radiation modes are associated with velocity distributions which radiate sound independently. The lowest-order radiation mode approximates the net volume velocity of the panel and can effectively be used as a control parameter at low frequencies. They also showed that the use of co-located sensors and actuators minimize the control spillover to higher frequencies and also results in a minimum phase system which can easily be incorporated in a feedback control scheme. Naghshineh and Mason [8] demonstrated acoustic control experimentally via volume velocity reduction using analog control methods to reduce the radiated sound of a circular plate. Their control scheme is primarily based on inverting the transfer function of the control loudspeaker. They showed that very close to the plate, volume velocity reduction may increase sound levels. However, rapid improvements are seen as one moves away from the panel. They also studied the use of multiple loudspeakers in an array and showed that

broadband sound reductions in the range of 10–20 dB can be achieved over a large spatial area, making the controller global in nature rather than just minimizing the sound pressure at a single microphone location. Burdisso and Fuller [9] developed a general algorithm for volume velocity cancellation using PZT actuators and PVDF sensors. Their study uses an optimization approach to determine a set of weakly radiating modes which become the desired response of the system, and calculate the control forces necessary to produce this response. It is interesting to note that the authors point out all the weakly radiating modes are non-volumetric, meaning the volume velocity of the modes is zero.

2. VOLUME VELOCITY APPROACH

A basic diagram of the control strategy is shown in Figure 1. It shows a segment of trim panel mounted to a stiffened fuselage skin via soft mounts to the struts. Each control segment of the panel is controlled by a single loudspeaker. A trim panel can be made up of many of these control segments, each having its control volume velocity provided by an integrated loudspeaker. The purpose of the loudspeaker is to produce a volume velocity which exactly cancels the volume velocity over the control segment. The volume velocity of each segment is sensed by an accelerometer array on the panel surface. The sample volume velocity profile on the right side of Figure 1 shows how the loudspeaker needs to be driven to cancel the surface's volume velocity. To cancel the volume velocity over the entire surface, the loudspeaker volume velocity should be equal in magnitude and opposite in phase to the panel volume.

By focusing on the total net volume velocity of the each control segment, an attempt can be made to minimize the component which radiates in a monopole-like fashion. At low frequencies, higher order radiators, such as dipoles and quadrupoles (which have a net volume velocity of zero) do not radiate sound nearly as efficiently as the monopole contribution. In this manner, the method works by controlling the component of the surface vibration which is radiating sound most efficiently.

The following analysis will show that, at low frequencies, volume velocity control directly minimizes the sound radiated to the far-field. Junger and Feit [10], among others,

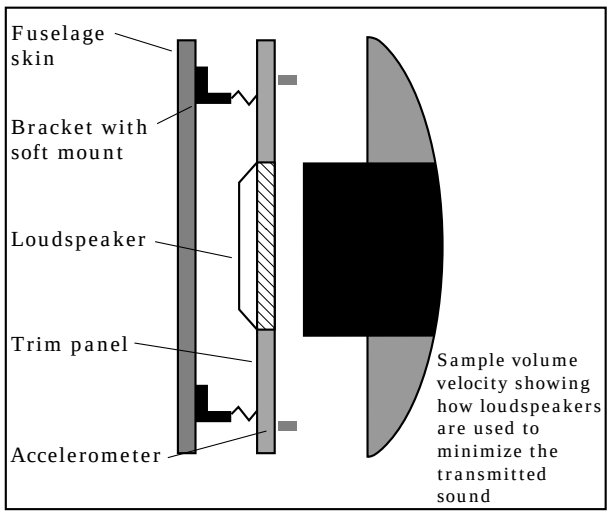

Figure 1. Volume velocity control diagram.

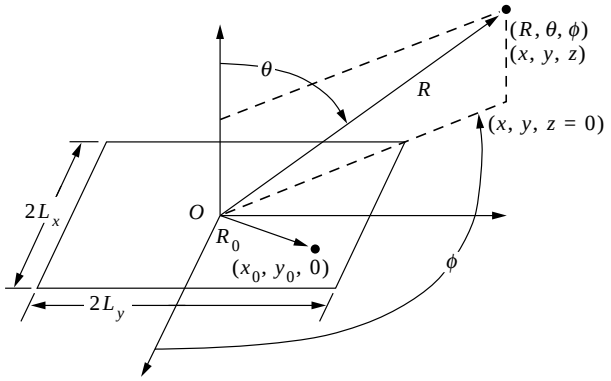

Figure 2. Construction of the far-field of a rectangular piston radiator, from Junger and Feit [10].

have developed the following general Rayleigh's formula for the sound pressure radiated by a vibrating rectangular panel:

$$p(R, \theta, \phi) = \frac{i\omega\rho\ \mathrm{e}^{ikR}}{2\pi R} \int_{-L_x}^{L_x} \int_{-L_y}^{L_y} \dot{w}(x_0, y_0)\, \mathrm{e}^{-ik \sin\theta(x_0 \cos\phi + y_0 \sin\phi)}\, \mathrm{d}x_0\, \mathrm{d}y_0 \tag{1}$$

where $p(R, \theta, \phi)$ is the radiated pressure; ρ is the density of air; $\dot{w}(x_0, y_0)$ is the velocity of the panel at the point (x_0, y_0), k is the acoustic wavenumber; and R, x_0, y_0, L_x, L_y, θ, and ϕ are defined in Figure 2. Equation (1) also assumes harmonic vibration with $\ddot{w} = i\omega\dot{w}$. This equation can be solved for the case of two uniform acceleration distributions for a square panel, one representing the vibration of the panel and one representing the control source as shown in Figure 3. The integral in the previous equation can be written as the sum of the three integrals by first using symmetry to only integrate over one-quarter of the panel, as shown by the dotted lines in Figure 3. The first is the integral for the control source ($\dot{w}_1$), the second is the integral of the panel ($\dot{w}_2$) over the entire area, including the

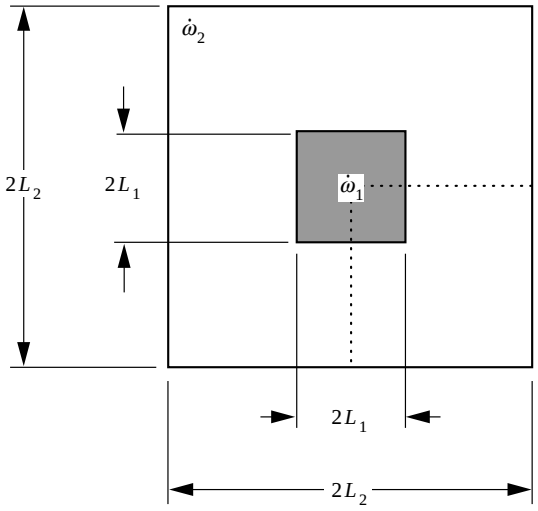

Figure 3. Panel and control source locations.

area of the control source. The third integral is used to subtract the control source area from the panel integral. The resulting equation is

$$p(R,\theta,\phi)=\frac{i2\omega\rho\ \mathrm{e}^{ikR}}{\pi R}\left(\int_0^{L_1}\int_0^{L_1}\dot{w}_1\ \mathrm{e}^{-ik\sin\theta(x_0\cos\phi+y_0\sin\phi)}\,\mathrm{d}x_0\,\mathrm{d}y_0\right.$$

$$+\int_0^{L_2}\int_0^{L_2}\dot{w}_2\ \mathrm{e}^{-ik\sin\theta(x_0\cos\phi+y_0\sin\phi)}\,\mathrm{d}x_0\,\mathrm{d}y_0$$

$$\left.-\int_0^{L_1}\int_0^{L_1}\dot{w}_2\ \mathrm{e}^{-ik\sin\theta(x_0\cos\phi+y_0\sin\phi)}\,\mathrm{d}x_0\,\mathrm{d}y_0\right). \tag{2}$$

Using a constant velocity profile, the configuration is even in both x_0 and y_0 and the complex Fourier transforms reduce to cosine transforms and can be written as

$$p(R,\theta,\phi)=\frac{2i\omega\rho\ \mathrm{e}^{ikR}}{\pi R}\left(\dot{w}_1\int_0^{L_1}\int_0^{L_1}\cos\gamma_x x_0\cos\gamma_y y_0\,\mathrm{d}x_0\,\mathrm{d}y_0\right.$$

$$+\dot{w}_2\int_0^{L_2}\int_0^{L_2}\cos\gamma_x x_0\cos\gamma_y y_0\,\mathrm{d}x_0\,\mathrm{d}y_0$$

$$\left.-\dot{w}_2\int_0^{L_1}\int_0^{L_1}\cos\gamma_x x_0\cos\gamma_y y_0\,\mathrm{d}x_0\,\mathrm{d}y_0\right), \tag{3}$$

where $\gamma_x = k\sin\theta\cos\phi$ and $\gamma_y = k\sin\theta\sin\phi$. Solving this equation yields

$$p(R,\theta,\phi)=\frac{2i\omega\rho\ \mathrm{e}^{ikR}}{\pi R}\left(\dot{w}_1\left(\frac{\sin\gamma_x L_1\sin\gamma_y L_1}{\gamma_x\gamma_y}+\dot{w}_2\frac{\sin\gamma_x L_2\sin\gamma_y L_2}{\gamma_x\gamma_y}-\dot{w}_2\frac{\sin\gamma_x L_1\sin\gamma_y L_1}{\gamma_x\gamma_y}\right)\right. \tag{4}$$

Remembering that γ_x and γ_y are both functions of k, it can be seen that at low frequencies, the values of γ_x and γ_y will approach zero. Therefore, at low frequencies, equation (4) can be written as

$$p(R,\theta,\phi)\approx\frac{2i\omega\rho\ \mathrm{e}^{ikR}}{\pi R}((\dot{w}_1-\dot{w}_2)L_1^2+\dot{w}_2 L_2^2). \tag{5}$$

To reduce the radiated pressure in the far-field, the expression in parenthesis should be set equal to zero, giving the following equation for the velocity of the control segment:

$$L_1^2\,\dot{w}_1=-(L_2^2-L_1^2)\dot{w}_2. \tag{6}$$

Looking at Figure 3, it can easily be seen that L_1^2 is simply the area of the control segment and that $L_2^2-L_1^2$ is the area of the panel (with the area of the control segment removed). Therefore, equation (6) states that the volume velocity of the control segment must be equal in magnitude and out-of-phase with the volume velocity of the panel to minimize the sound pressure radiated into the far-field. It is this simple physical argument that forms the basis of our control algorithm. The effects of volume velocity control in the near-field of the source was analyzed by St. Pierre [11] and it was found that any sound pressure

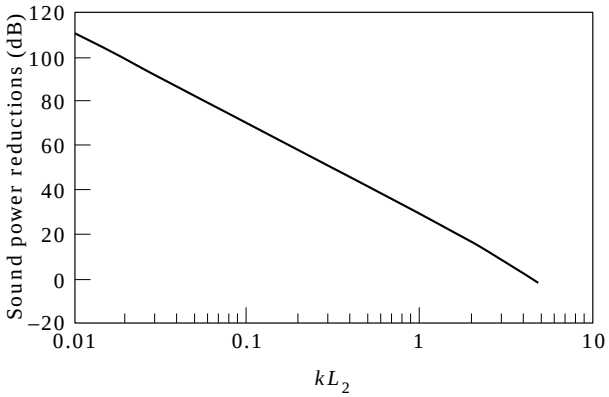

Figure 4. Sound power reduction (dB re 10^{-12} W) as a function of frequency.

increases were less than 4 dB and were confined to a small area in the near field of the control loudspeaker.

2.1. FREQUENCY LIMITS OF VOLUME VELOCITY CONTROL

The previous derivation assumed a very low frequency sound source, with $kL_2 \ll 1$. Physically, this means that the wavelength of sound in air is much longer than the length of the panel. It also means that the pressure field caused by the vibration of the panel is nearly constant at a given radius from the center of the panel in the far field, and the pressure field is independent of both θ and ϕ (see Figure 2). This section will discuss how moving to higher frequencies affects the performance of volume velocity control and will determine an upper frequency limit for using this control strategy.

To determine the efficiency of volume velocity control versus frequency, a measure of effectiveness needs to be determined. Using pressure (as was done for kL_2) is not sufficient at higher frequencies because the pressure field is no longer constant for a given radius. Therefore, sound power was used in this study as the measure of effectiveness. Junger and Feit [10] give the following equation for the sound power radiated by a source on an infinite baffle:

$$\Pi = \frac{R^2}{2\rho c} \int_0^{2\pi} \int_0^{\pi/2} |p(R, \theta, \phi)|^2 \sin\theta \, \mathrm{d}\theta \, \mathrm{d}\phi, \qquad kR \gg 1. \tag{7}$$

This equation simply integrates the sound pressure over a large hemisphere of radius R that is concentric with the sound source. Substituting equation (4) for the pressure, equation (7) can then be solved for the total radiated sound power. This integration was done numerically using the *Mathematica* computer package. The sound power, for various values of kL_2, was determined for two separate conditions. The first was with no control source, i.e., $\dot{w}_1 = 0$, and the second was for a control source amplitude given by equation (6). The difference between the two is the sound power reduction that volume velocity control can achieve. For $R = 100$ m, $\dot{w}_2 = 1$ m/s, $L_1 = 0{\cdot}3\, l_2$, the results of the analysis are shown in Figure 4, which clearly shows a logarithmic decrease in the sound power reduction possible as frequency increases. Above a kL_2 of 3 or so, the maximum sound power reduction using volume velocity control is under 10 dB. For practical implementations, this is the upper limit in frequency for which volume velocity control can

be used with confidence. Therefore, the maximum frequency (in Hz) at which volume velocity control can be used is given by

$$f = (3/2\pi)\,(c/L_2). \tag{8}$$

Thus a 0·30-m (1 ft) square panel can effectively control up to a frequency of approximately 540 Hz using the volume velocity cancellation technique.

3. EXPERIMENTAL PANEL DESIGN

To match the previous analytical work as closely as possible, a panel segment design was desired that, in the frequency band of interest, vibrated either like a piston, or in its first mode of vibration. In this way, only one accelerometer would be necessary to estimate the volume velocity. Such a design, fabricated by PCB Piezotronics (Depew, NY) is shown in Figure 5. The panel consists of four segments of composite panel separated by an aluminum grid. Each segment is made of two glass epoxy sheets with an aluminum honeycomb core. These four control segments are separated from the aluminum frame by thin layer of RTV silicone/rubber isolation which serves as a vibration isolation mechanism. These control segments are independent from each other, connected only by the aluminum frame.

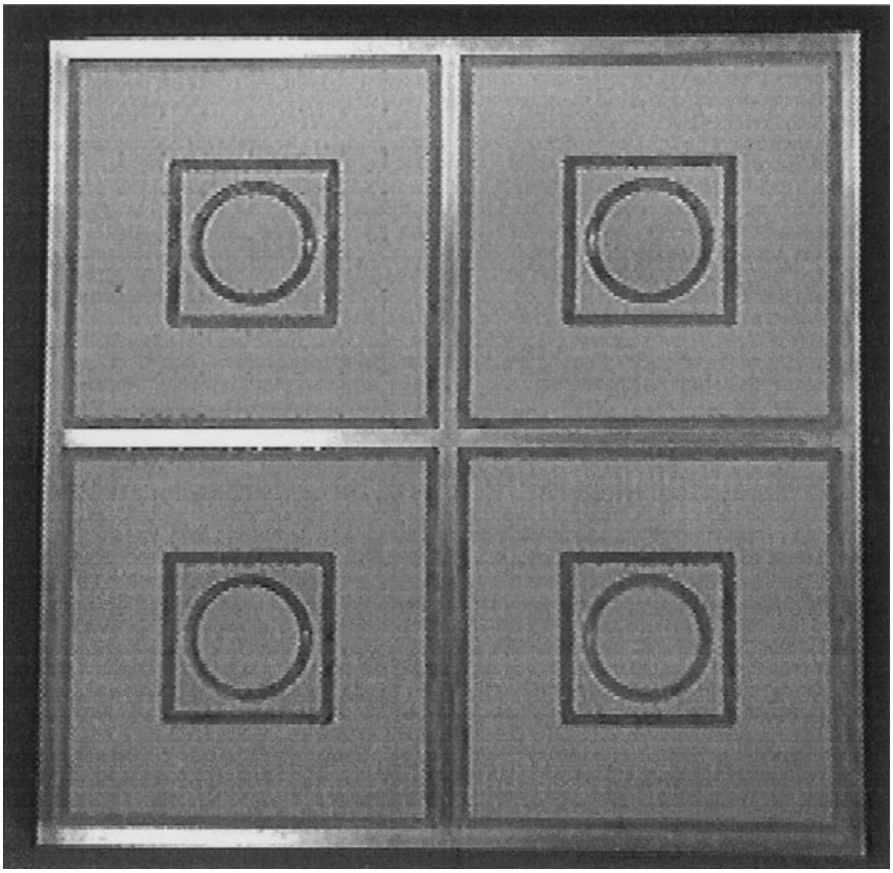

Figure 5. Panel design.

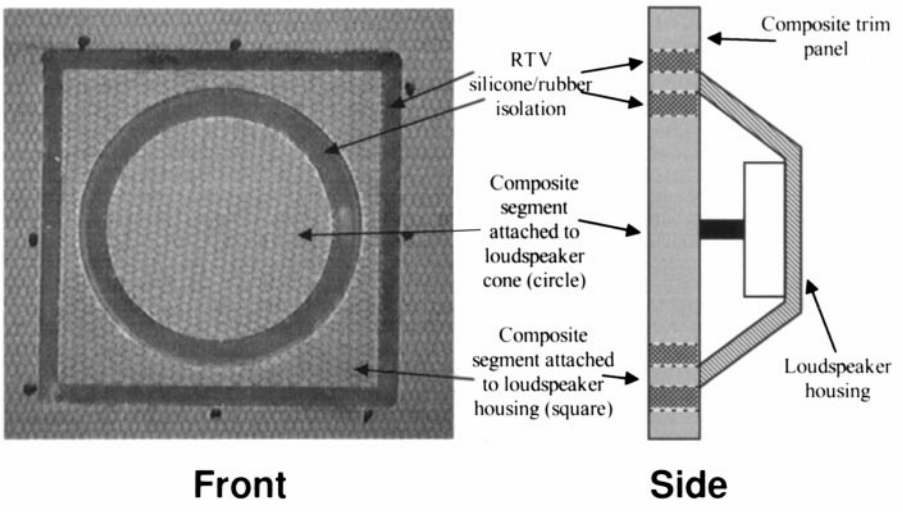

Figure 6. Control loudspeaker design.

The main feature of each panel segment is the loudspeaker imbedded into the panel. The purpose of this loudspeaker is to produce a volume velocity which will cancel that caused by the vibration of the panel surrounding it. A close-up of the loudspeaker design is given in Figure 6. The side view of the panel shows the loudspeaker attachment. The loudspeakers chosen were lightweight, but capable of producing the sound levels necessary at the control frequencies.

Separating the various elements within each segment is a thin layer of RTV silicone/rubber material (manufactured by General Electric) approximately 3/8 in. wide. These layers serve to isolate the vibration of the loudspeaker from the panel since cross-talk between the control loudspeaker and the panel itself is problematic, as will be discussed. A measure of the effectiveness of the RTV isolation is given in Figure 7. The measurement labeled "inside RTV isolation" is the transfer function of an accelerometer (placed on the outer square-shaped segment of trim panel) to the white noise input to the loudspeaker. The meaurement labeled "outside RTV isolation" is the transfer function for an accelerometer placed on the panel adjacent to the location of the first measurement. As can be seen, the isolation works very well in the range of 100–400 Hz, with ≈ 20 dB reduction (in terms of acceleration). It should also be noted that the range around -40 dB represents the noise floor when the readings were taken. Therefore, it can be concluded that, in this frequency range, the panel response is minimally affected by the sound produced by the control loudspeaker.

A modal analysis of one segment of the segmented panel was conducted to determine the natural frequencies and mode shapes at low frequencies. To do this, the segment was divided into a 9×9 grid of measurement points. Measurements were only taken on the outer square composite panel. The analysis was done using a modal impact hammer and a stationary accelerometer. Figure 8 shows a representative frequency response plot along with two mode shapes. The first resonance at 31 Hz appears to be a simple piston-like motion of the panel. The mode shown on the left in Figure 8 occurs at 83 Hz and is a rocking type mode about one corner of the panel. The first real structural mode of the panel itself occurs at 422 Hz and is shown on the right side of the figure. It can be seen that the unusual boundary conditions complicate the panel response. However, as we

discuss in the next section, this does not affect the method for sensing the volume velocity of the segment.

It would appear from the data presented in the previous section that sensing the volume velocity of each segment would again be a difficult task. The appearance of low frequency rigid-body modes caused by the boundary conditions may cause rocking of the panel, thus necessitating an array of accelerometers to obtain an accurate measurement of the volume velocity. This, however, is not the case. In the control strategy pursued in this study, the panel is not excited structurally, but rather acoustically by plane waves exciting one side of the panel. For this type of forced response, the forcing function causes the modal response to be mainly a piston-like motion. It should also be noted in Figure 8 that in the frequnency range of 150–300 Hz, there is a noticeable absence of strong resonances and the panel is vibrating off-resonance.

Measurements in a transmission loss chamber were taken of the panel vibration excited by a sinusoidal acoustic source in the source room. The acceleration, shown in Figure 9 for a frequency of 200 Hz, was measured at various points around the panel. The results are shown in relation to the point marked "1" (shown with a magnitude of 1·0 and a phase of 0°). This point is the location of the permanent accelerometer used in the control strategy. The key observation is that it is apparent the panel's surface is generally moving in phase. The two corner measurements do have phase differences of around 30° but they were the largest seen in any measurement, even at other frequencies in the 150–300 Hz band.

This leads to the conclusion that only one accelerometer (located at the reference position in Figure 9) is necessary to get an accurate measurement of the volume velocity. The next section will detail the control strategy used for the segmented panel with one accelerometer.

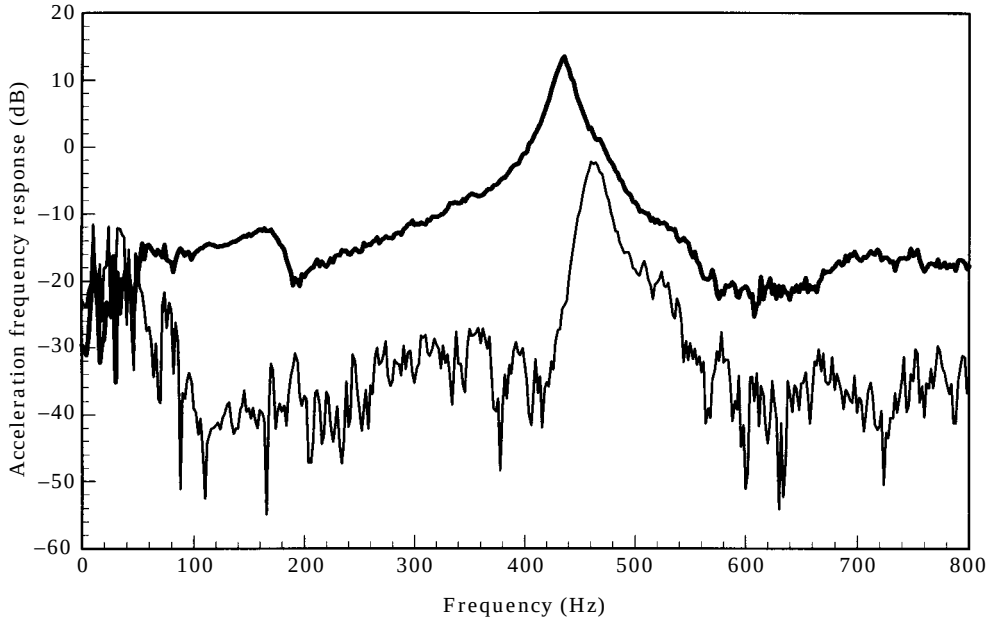

Figure 7. Vibration isolation of control loudspeaker; —, inside RTV isolation; —, outside.

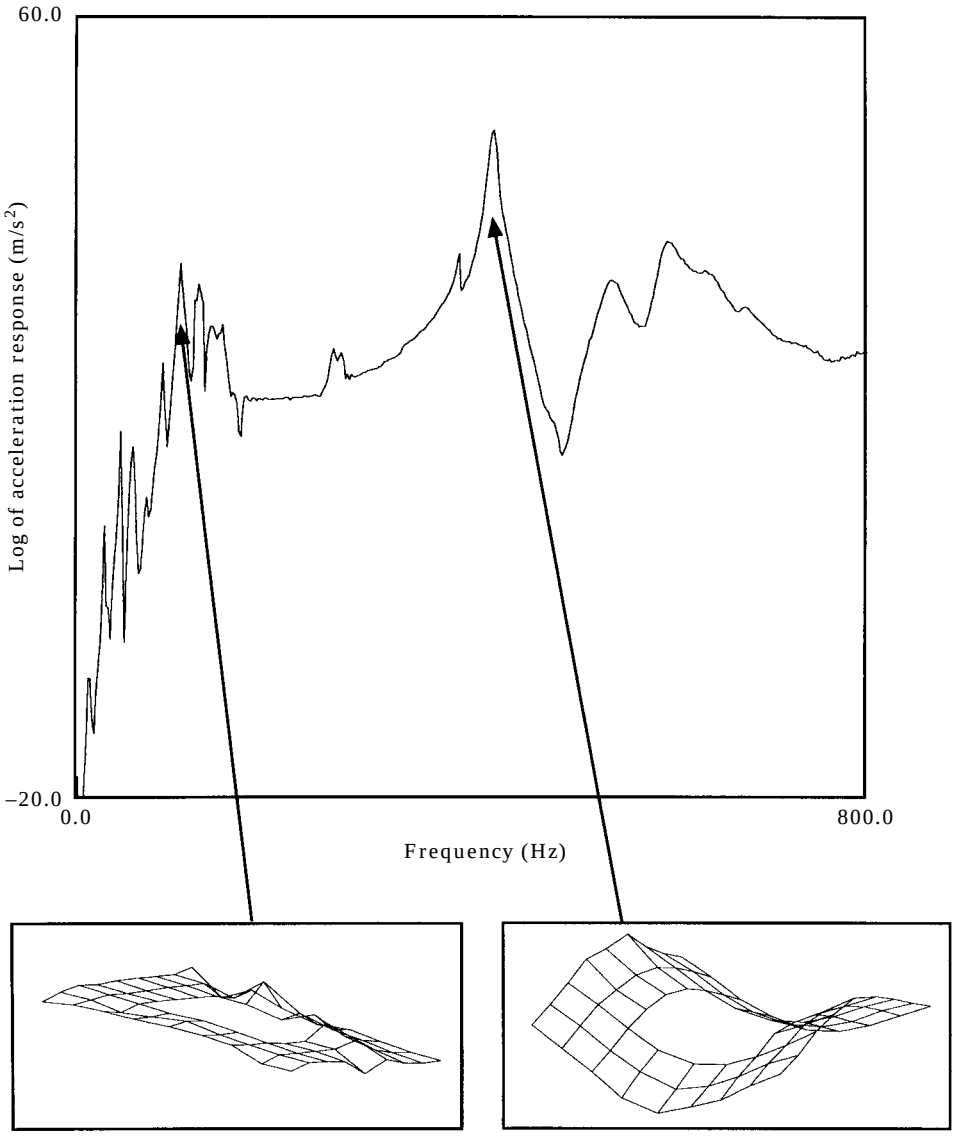

Figure 8. Modal analysis results for segmented panel.

3.1. PANEL CONTROLLER

The basics of the filtered-X LMS algorithm is fully described by Kuo and Morgan [12] and is the control algorithm used in this work. There are two accelerometers for each control segment, one located on the panel and another located on the control loudspeaker. Since the error signal to be minimized in the LMS algorithm is the total volume velocity of the segment, the two accelerometer readings give us an exact measurement of that error. Because of this, the filtered-X LMS algorithm takes on a slightly different form as shown in Figure 10. Notice first that the error signal is defined as

$$e(n) = z(n) - \frac{A_{panel}}{A_{loudspk}} x(n), \tag{9}$$

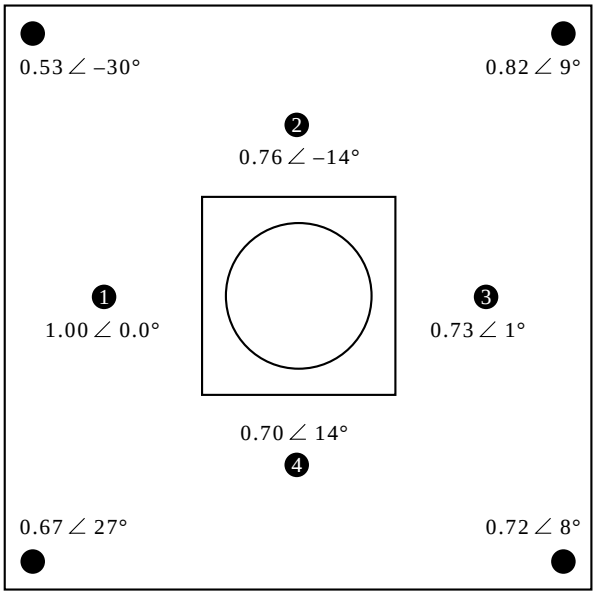

Figure 9. Test results for vibration of segmented panel at 200 Hz.

where $z(n)$ is the acceleration measurement of the loudspeaker, $x(n)$ is the acceleration measurement of the panel, and the ratio of panel area to loudspeaker area is the proportionality constant.

It can also be noted that since there is an exact measurement of the error function available, no need for an estimate of the loudspeaker transfer function is necessary. This would tend to indicate that the filtered-X algorithm is unnecessary. However, as Figure 10 shows, by inserting a pure delay filter which approximates the delays apparent in the hardware in place of the plant estimate, a more stable and faster converging algorithm is produced. The nature of these delays and their impact on control will be described later. Also, the filtered-X algorithm works best when the feed-forward signal (in this case the panel acceleration) is purely a reflection of the disturbance and not influenced by the control signal. This is why the RTV isolation of the loudspeaker is so important in this implementation.

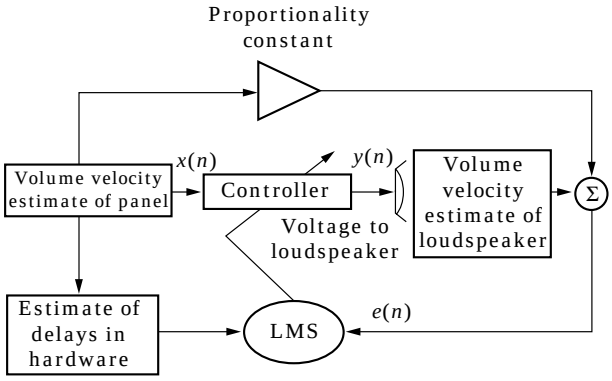

Figure 10. Control algorithm used for segmented panel.

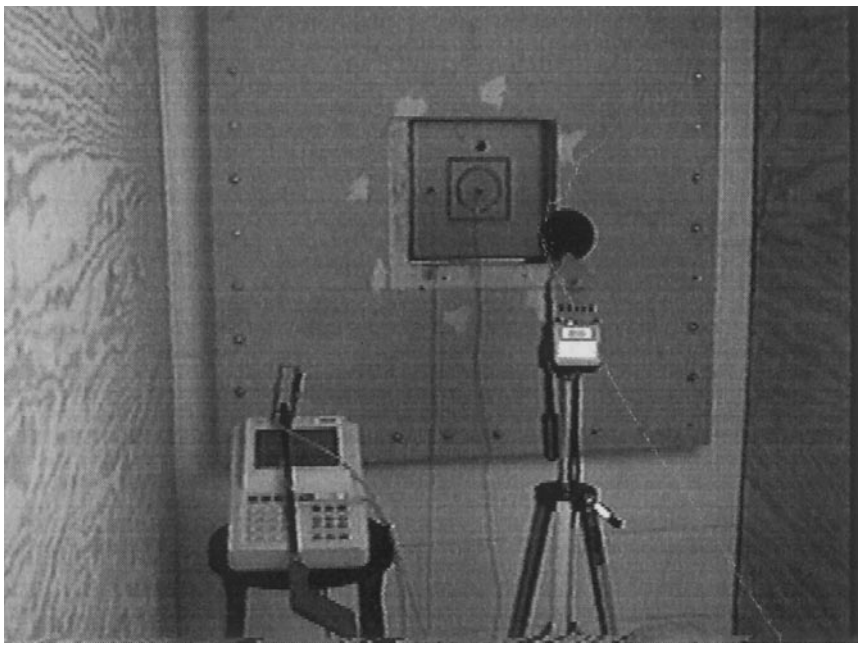

Figure 11. Picture of segmented panel in transmission loss window from receiver room.

3.2. EXPERIMENTAL SET-UP

For test purposes, one control segment of the panel was isolated in the transmission loss window as shown in views from the receiver room in Figure 11. This was done by filling the rest of the transmission loss window with thick layers of plywood to ensure that sound only radiated from the trim panel. Care was taken to minimize this effect by solidly mounting the test panel in the window and sealing any air gaps with clay.

The set-up for the source room of the transmission loss chamber consisted of a Brüel and Kjær (B&K) Type 1024 signal generator, a Biamp Model 2500 high performance amplifier and two Soundtech CX2 240 W speakers with a rated low frequency limit of 40 Hz. This set-up is more than adequate for delivering the high sound levels (up to 110 dB) at low frequency necessary to conduct the transmission loss experiments. The signal generator used is capable of producing a variety of signals, including pure sine waves, sine waves warbled over a frequency band, and random noise over a variety of frequency ranges.

The easiest and most reliable method available to measure the sound power radiated by a vibrating surface is to measure the magnitude of the intensity, $I(\omega)$, in a plane just above the surface. To do this, a B&K two-microphone intensity probe is used. The intensity is then related to power by

$$W = \int_S I_n(\omega)\,\mathrm{d}S, \tag{10}$$

where $I_n(\omega)$ is the value of the intensity normal to the surface.

This integration over the surface was accomplished by scanning the vibrating surface of the panel segment with the intensity probe via a HP3569A analyzer which was programmed to display sound power in 1/3 octave bands.

As described earlier, only one accelerometer is needed to estimate the volume velocity of the panel. An accelerometer is also placed on the loudspeaker to measure its volume velocity. After passing through an accelerometer power supply, each signal is filtered through a high-pass and low-pass ITHACO filter set at 200 Hz for the high-pass filter and 315 Hz for the low-pass filter. These filters, as will be shown in the following section, were necessary to control some feedback encountered in implementing control over a frequency band instead of a discrete frequency. Each of the signals was then passed through a B&K Measuring Amplifier so that as much of the working range of the analog-to-digital board on the PC was used without risking saturating the board and clipping the signal. The input range of the analog-to-digital board was $\pm 2{\cdot}5$ V. The amount of amplification was measured and used as an input to the control program so that the original accelerometer signal is known to the program. The entire computer control process is described in the next section. The output from the computer is then passed through a power amplifier and sent to the control loudspeaker. Again, the change in signal magnitude caused by the amplifier is an input to the controller. The phase lag caused by the amplifier is also taken into account.

The control board used is a Spectrum MDC40S board using a Texas Instruments TMS320C40 DSP chip. The control program begins by initializing the DSP board as well as the A/D and D/A boards along with allocating memory needed for the filters. The program then retrieves the sampled signal from the accelerometer mounted on the speaker and the accelerometer mounted on the panel from the analog-to-digital board. The error function for the LMS algorithm is then computed using

$$e(n) = A_{spk} * u_{spk}(n) + A_{pan} * u_{pan}(n), \tag{11}$$

when $e(n)$ is the error for the nth sample, A_{spk} and A_{pan} are the areas of the speaker and panel, respectively, and $u_{spk}(n)$ and $u_{pan}(n)$ are the voltage of the speaker and panel accelerometers as sampled by the A/D board, respectively.

The panel signal is then filtered through the pure delay filter with the output being the input to the LMS adaptive algorithm. The error function just defined is used to adjust the controller weights. The panel input is then filtered by the controller weights, with the output being the voltage sent to the loudspeaker through the digital-to-analog board.

4. EXPERIMENTAL RESULTS

The results presented here will be for two test cases. The first is for a 230-Hz pure tone input while the second case warbles that tone between 200 and 260 Hz. For each case, sound power measuread via the two-microphone intensity probe is used to measure the effectiveness of the controller. Since the analyzer calculates sound power in 1/3-octave bands, the sum of the sound power in the 200- and 250-Hz 1/3-octave bands is used to determine the control effectiveness within the excitation band.

4.1. RESULTS FOR 230 HZ EXCITATION

The test was originally conducted at a single frequency to verify that the control algorithm was operating as expected. The results show that a 22-dB reduction in sound power was noted in the 200- and 250-Hz 1/3-octave bands for this case, from 75 dB to 53 dB. At a frequency of 230 Hz, the value of kL_2 is approximatley 1·3. Referring to Figure 4, the maximum sound power reduction we would expect is around 30 dB. Therefore, this result is in the range expected for volume velocity control.

The reductions obtained were easy to hear in the receiver room of the transmission loss chamber. The controller very quickly locked onto the excitation frequency and achieved

control. For this simple case, control was achieved within a few seconds and the controller remained stable throughout the measurement process. The effectiveness of the controller was measured by using a HP35660A Dynamic Signal Analyzer to measure the transfer function between the two accelerometer readings. The object of the controller is to make these two signals exactly out of phase and with an appropriate magnitude difference equal to the ratio of the surface areas of the panel and the loudspeaker. By displaying the magnitude and phase of the transfer function between the two accelerometer readings on the signal analyzer, the effect of the controller could easily be seen. For the dimensions of the test panel, the ratio of the two surface areas is 14·9; therefore we would expect to see this relationship between the accelerometer readings during control. Figure 12 shows the frequency response, both magnitude and phase, of the loudspeaker acceleration to the panel acceleration after control. This shows that the sound power reductions measures were the result of using volume velocity control, i.e., the observed phase difference is 180° and the magnitude ratio is ≈ 15. The spectra of the two accelerometer readings both before and after control are given in Figure 13. They show that control is achieved without substantially changing the vibration of the panel itself, except for slight increases at harmonics of the forcing frequency caused by non-linearities in the loudspeaker itself.

The results of the sound power measurements over a broad frequency range are shown in Figure 14. The reductions in the 200- and 250-Hz third-octave bands match up well with the acceleration data shown and it appears that this method achieves significant acoustic control at single frequencies.

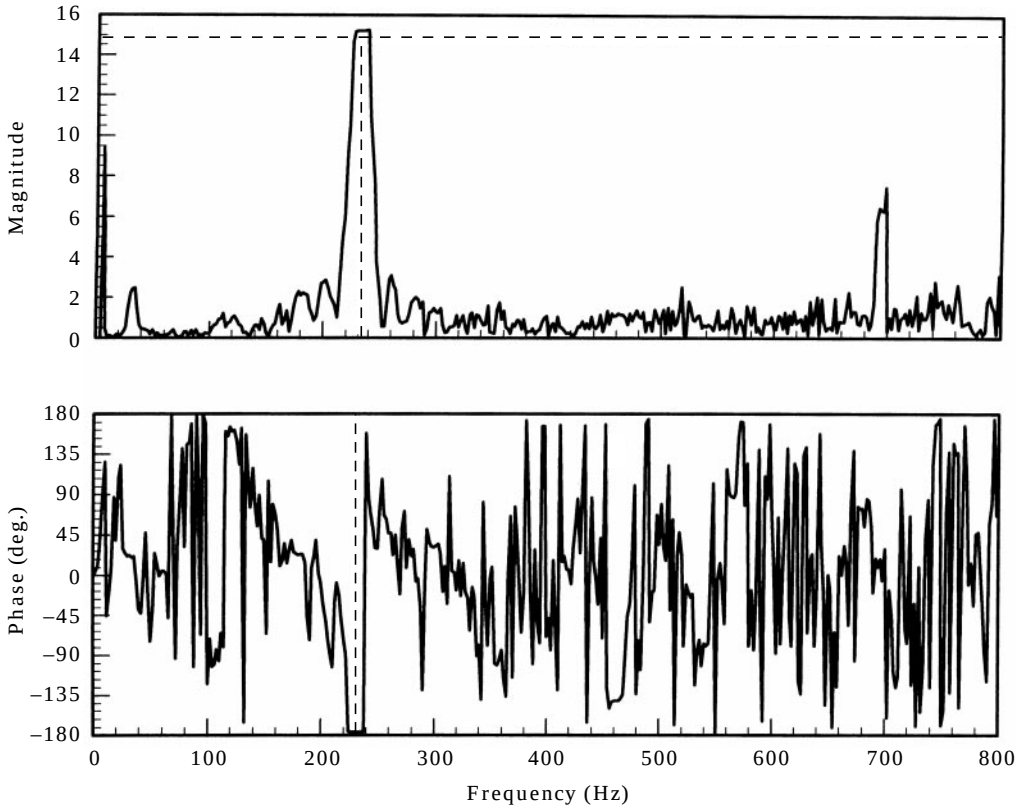

Figure 12. Frequency response of measured loudspeaker acceleration to panel acceleration after control at 230 Hz (control frequency denoted by dashed line).

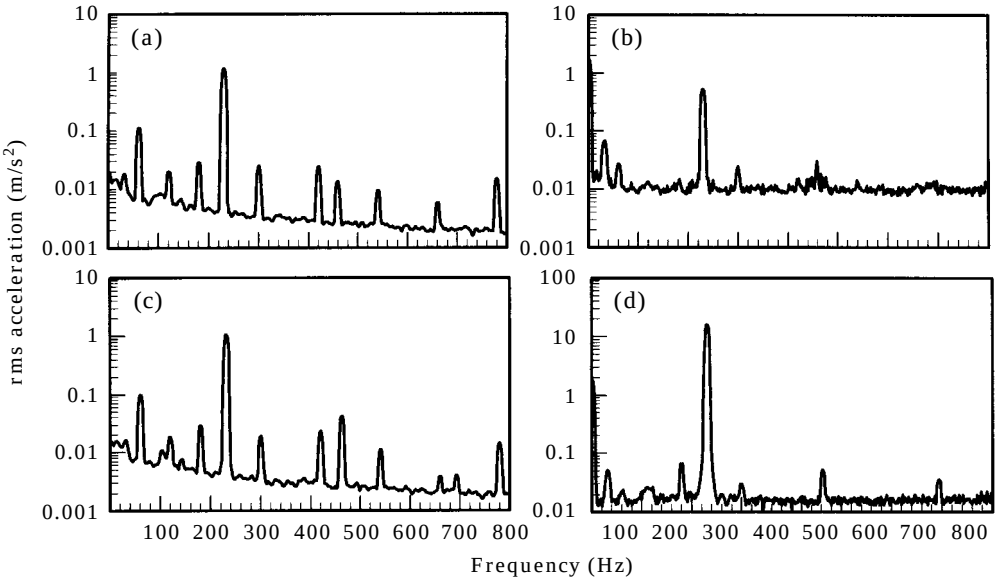

Figure 13. Spectra of acceleration readings for (a) and (c) panel (left) and (b) and (d) loudspeaker (right); both (a) and (b) before (top), and (c) and (d) after (bottom) control for 230 Hz case.

4.2. RESULTS WITH 200–260 HZ WARBLED TONE EXCITATION

When moving to control over a range of frequencies, it was decided to use a warbled sine wave as the input to the source room, created by the B&K Type 1024 signal generator. It should be noted that the rate of frequency change was fast enough that the controller could not track the frequency. This means that the controller was working in a broad-band sense and not simply as single frequency controller. This was confirmed by observing the transfer function between the accelerometer signals shown in Figure 15. Once the controller converged (and this took around 30 s for this case), a phase shift of 180° can be observed for the upper part of the frequency range, with some degradation at the lower end of the frequency band. The magnitude plot showed a similar consistency, although a greater variation can be seen in this result since the controller was adapting to input over the entire frequency range and not just at a single frequency.

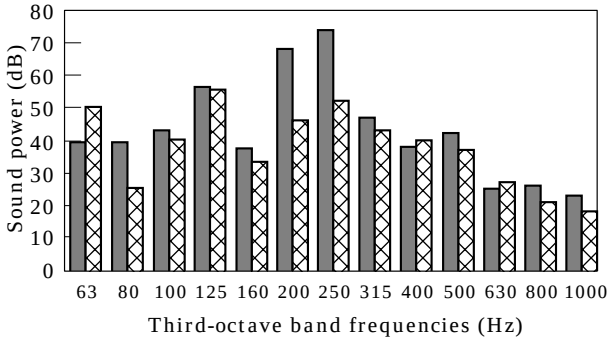

Figure 14. Sound power results for 230 Hz test case on segmented panel (dB re 10^{-12} W); ■, without control; ⊠, with control.

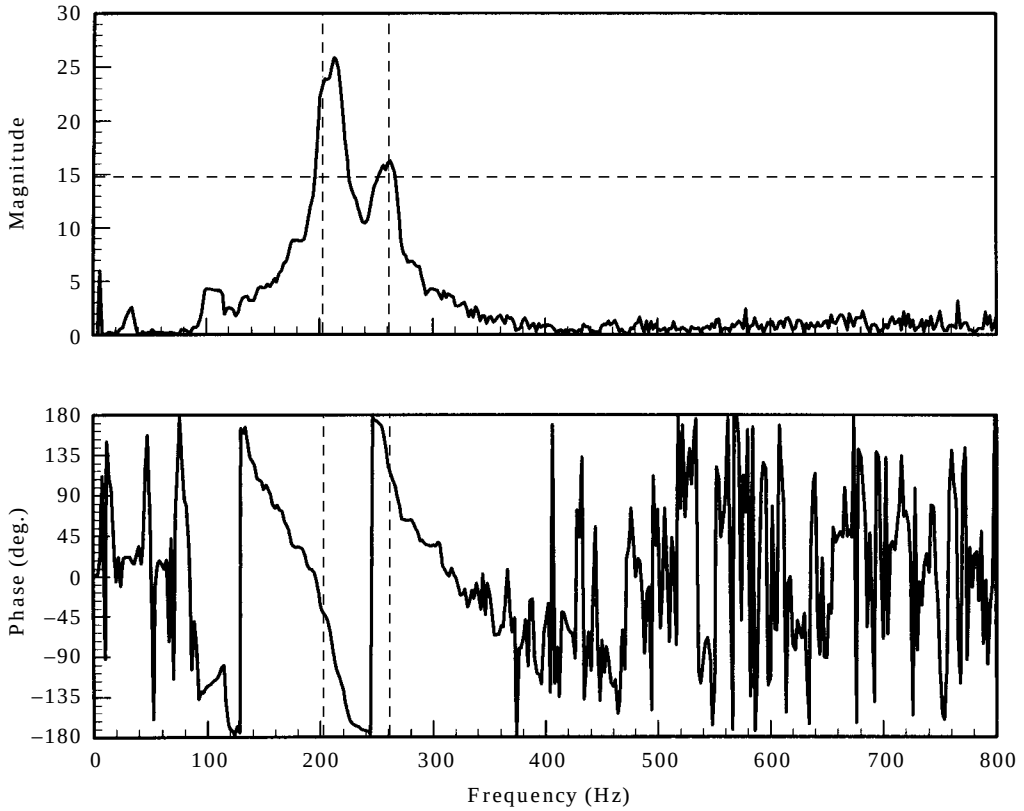

Figure 15. Frequency response of measured loudspeaker acceleration to panel acceleration after control between 200 and 260 Hz (control range denoted by dashed lines).

The results for this case (Figure 16) show a 9-dB reduction in sound power over the band, from 70 to 61 dB. The sound reductions occur in the frequency band of excitation, but some increases in sound power both above and below this frequency range are also observed. These can also be explained by observing the acceleration spectra both before and after control, as shown in Figure 17.

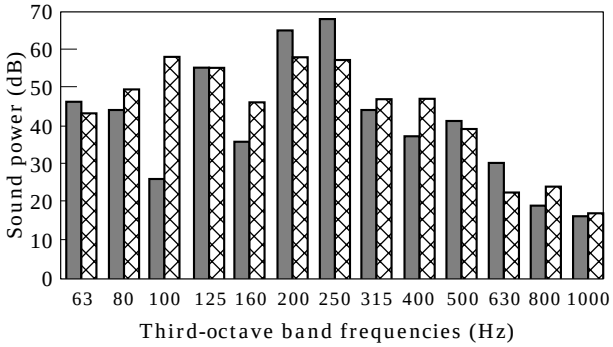

Figure 16. Sound power results for 200–260 Hz test case on segmented panel; ■, without control, ⊠, with control.

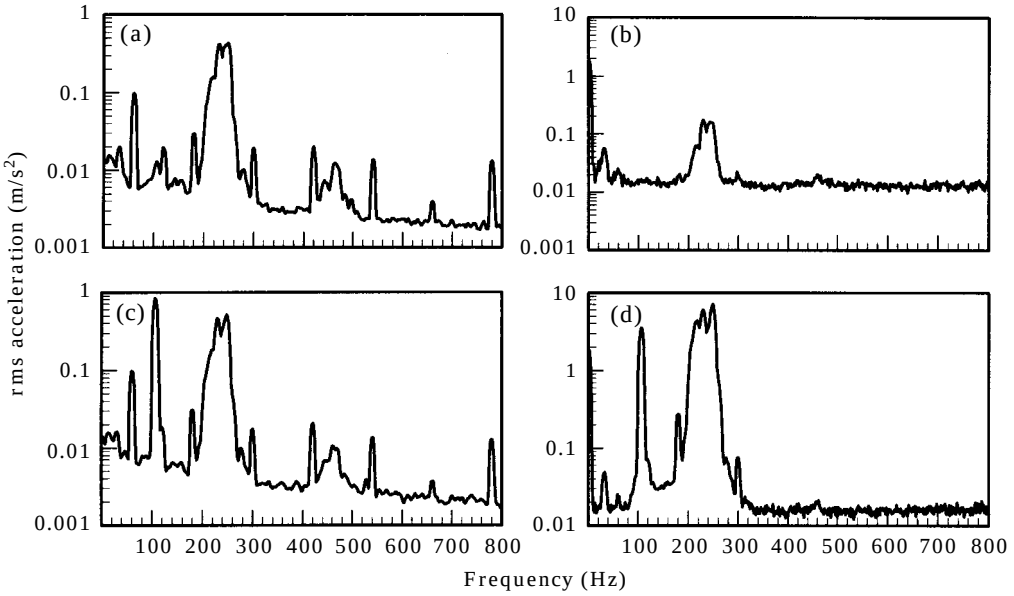

Figure 17. Spectra of acceleration readings for (a) and (c) before (top) and (c) and (d) after (bottom) control for 200–260 Hz case.

The increases at higher frequencies, most notably in the 400-Hz third-octave band are mainly caused by non-linearities in the control loudspeaker. To achieve the sound levels needed for control, the loudspeaker was pushed to its linear limit. When warbling the sine wave for this experiment, the amplitude of the input sound source varied with time and at certain intervals was high enough to cause a non-linear response by the control loudspeaker. This caused harmonics of the response heard as short "chirps" at varying intervals. These "chirps" were picked up by the intensity probe during the measurement and caused the increases at higher frequencies.

Below the excitation frequency range, the main increase is seen in the 100-Hz third-octave band. This increase is substantial and, in effect, masks out the reductions seen in the test frequency band. Figure 17 offers an explanation for this anomaly. Significant vibration levels are present at a single frequency just above 100 Hz both on the panel and loudspeaker. Recall from Figure 8 the modal analysis done on the segmented panel. Rigid body modes occur at low frequencies near 100 Hz and in all probability one of those strong resonances, like the rocking mode pictured at the bottom of the figure, is being excited by either the non-linear response of the loudspeaker or some other non-linearity in the system. This vibration is then detected by the accelerometer on the panel and contaminates the control system. While the loudspeaker is not capable of efficiently producing sound at this frequency, it can still vibrate at this frequency. The low-frequency vibrations are not fully attenuated by the RTV so this excitation by the loudspeaker transmits back to the panel to keep it resonating at this frequency (see Figure 7). Practically, this low frequency vibration eventually increased to the point where either the input or output signals to the controller were being clipped, causing harmonic distortion and instability. To circumvent this problem, a high pass filter was added to the analog pre-processing of the accelerometer signals to help control this low-frequency feedback. However, while the filter did reduce the response, it was not able to eliminate it totally. One method for dealing with this problem is to identify exactly which mode of vibration of causing the resonance.

For example, if it is a rocking mode, it would be possible to add an accelerometer to the panel such that the two panel accelerometers, when summed, cancel out the response of this mode. Thus, this vibration would not be fed back into the system. In our application, only one accelerometer was used because the assumption was made of piston-like vibration. However, if non-linearities excited other unwanted modes of vibration, these could be dealt with by using a small array of accelerometers configured as modal filters.

5. NUMERICAL ANALYSIS

Based on the data presented earlier, it can be assumed that the panel was responding to the acoustic excitation in a piston-like manner. Because of this, the simple equations developed earlier can be used to estimate the sound power radiated by the physical panel both with and without control. To do this, the accelerometer spectrum data given previously was used in equation (4) to determine the sound pressure and equation (7) was then used to compute the sound power. Because the measured data is acceleration data, Equation (4) was modified to the form

$$p(R, \theta, \phi) = \frac{2\rho\, e^{ikR}}{\pi R}\left(\ddot{w}_1 \frac{\sin \gamma_x L_1 \sin \gamma_y L_1}{\gamma_x \gamma_y} + \ddot{w}_2 \frac{\sin \gamma_x L_2 \sin \gamma_y L_2}{\gamma_x \gamma_y} - \ddot{w}_2 \frac{\sin \gamma_x L_1 \sin \gamma_y L_1}{\gamma_x \gamma_y}\right), \tag{12}$$

where $\ddot{w}_1$ is the acceleration of the loudspeaker and $\ddot{w}_2$ is the acceleration of the panel. This equation assumes that the panel's acceleration is given by the accelerometer measurement at a single point and similarly with the loudspeaker. This assumption will highlight what effect any rocking motion may have on the overall effectiveness of the controller.

For the single frequency test at 230 Hz, the simulation was done only at the excitation frequency. The measured acceleration data predicts a 22-dB reduction in sound power which exactly matches that measured. Thus, we conclude that for this case, the panel was vibrating in a near perfect piston mode.

For the case of a warbled tone between 200 and 260 Hz, the sound power was numerically calculated every 2 Hz in the excitation bandwidth. The results are given in Figure 18. For the entire band, the sound power before control was 73 dB and after control 68 dB. This means a 5-dB sound power reduction is predicted, and a 9-dB sound power

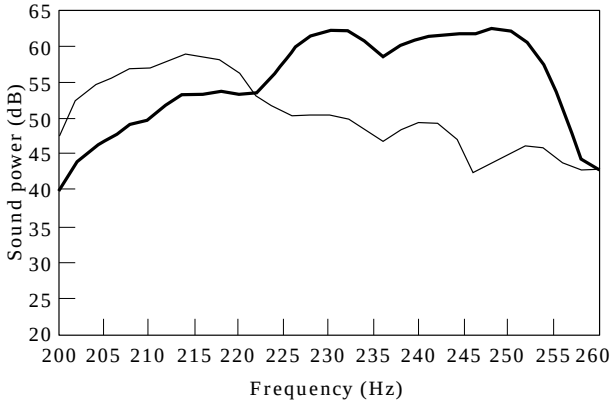

Figure 18. Numerical sound power results for 200–260 Hz case (dB re 10^{-12} W); —, without control; —, with control.

reduction was measured using the intensity probe. There are several reasons for the controller's difficulty at the lower end of the frequency band. Foremost is the fact that the uncontrolled sound power levels are lower for this range. The low excitation levels for the lower portion of the band are most likely due to a combination of the panel's response and the input signal provided by the signal generator. Volume velocity control will still yield reductions for this area, however, the controller first controlled the stronger radiating portions and had not completely adapted to control the lower frequencies when the spectrum data was taken. Long delays between starting the controller and taking the data (to allow for the controller to completely adapt) were not possible in this case due to the eventual instability caused by the low frequency vibration. This also explains why the experimental data showed 9 dB of sound reduction while the numerical data showed only a 5-dB reduction. The spectrum data was taken from the analyzer prior to the sound intensity measurements. Therefore, the adapter had effected better control on the low frequency region by this time and the overall controller performance was improved.

6. CONCLUSIONS

A successful method for controling sound transmitted by vibrating panels has been presented. It is based on locally controlling the volume velocity over one portion of the panel, called a control segment. An integrated control loudspeaker produces a volume velocity which is equal in magnitude to an out of phase with the segment's volume velocity. In this way, the sound intensity is minimized at the source, provided that the volume velocity condition is met.

Building on first principles, it was demonstrated that, in the low frequency limit, the sound pressure could be completely canceled at the surface using this method for a piston-like source, leading to complete elimination of sound in the far-field. It was also shown that volume velocity control worked at frequencies up to a kL of $\approx 3{\cdot}0$, where a 10-dB reduction in sound power could be obtained. At frequencies above that, the panel segments would have to be made smaller to effect adequate reductions. The digital control system developed for this approach is a variant on the classic, filtered-X, feed-forward algorithm and relies solely on vibration information from the panel for control.

The work reported in this paper has demonstrated both analytically and experimentally how localized volume velocity control might be implemented in practical applications. The two applications discussed most frequently have been in the interior acoustic control of turbo-prop aircraft and helicopters. It is certainly conceivable that this strategy could be employed wherever it is necessary to control the low frequency sound transmitted by a vibrating structure. Such applications include large power transformers and other heavy machinery. A wide variety of active control problems could be tackled using this simple, yet effective, control method.

REFERENCES

1. J. F. Wilby 1996 *Journal of Sound and Vibration* **190**, 545–564. Aircraft interior noise.
2. B. S. Murray and J. F. Wilby 1978 *Proceedings of an International Specialists Symposium held at NASA Langley Research Center, Hampton, VA, NASA Conference Publication* 2052. Helicopter cabin noise—methods of source and path identification and characterization.
3. R. L. Clark and C. R. Fuller 1992 *Journal of Intelligent Material Systems and Structures* **3**, 296–315. Active structural acoustic control with adaptive structures including wavenumber considerations.
4. R. L. Clark and C. R. Fuller 1992 *Journal of the Acoustical Society of America* **92**, 1521–1533.

Optimal placement of piezoelectric actuators and polyvinylidene fluoride sensors in active structural acoustic control approaches.
5. R. L. Clark and C. R. Fuller 1992 *Journal of the Acoustical Society of America* **92**, 1534–1544. A model reference approach for implementing active structural acoustic control.
6. K. Naghshineh and G. H. Koopmann 1992 *DSC-Vol*. 38, *Active Control of Noise and Vibration*, 23–31. An active control strategy for achieving weak radiator structures: single frequency and ergodic random excitations.
7. M. E. Johnson and S. J. Elliott 1995 *Journal of the Acoustical Society of America* **98**, 2174–2186. Active control of sound radiation using volume velocity cancellation.
8. K. Naghshineh and V. B. Mason 1996 *Applied Acoustics* **47**, 27–46. Reduction of sound radiated from vibrating sources via active control of local volume velocity.
9. R. A. Burdisso and C. R. Fuller 1994 *Journal of the Acoustical Society of America* **96**, 1582–1591. Design of active structural acoustic control systems by eigenproperty assignment.
10. M. C. Junger and D. Feit 1993 *Sound*, *Structures*, *and Their Interaction*. New York: Acoustical Society of America.
11. R. L. St. Pierre 1997 *PhD Dissertation*, *The Pennsylvania State University*. Volume velocity control of sound transmission through composite panels.
12. S. M. Kuo and D. R. Morgan 1996 *Active Noise Control Systems—Algorithms and DSP Implementations*. New York: Wiley.